Chromatin Remodeling Proteins Interact with Pericentrin to Regulate Centrosome Integrity☒ ☒

James Edward Sillibourne,* Bénédicte Delaval, Sambra Redick, Manisha Sinha, and Stephen John Doxsey

Program in Molecular Medicine, University of Massachusetts, Worcester, MA 01605

Pericentrin is an integral centrosomal component that anchors regulatory and structural molecules to centrosomes. In a yeast two-hybrid screen with pericentrin we identified chromodomain helicase DNA-binding protein 4 (CHD4/Mi2β). CHD4 is part of the multiprotein nucleosome remodeling deacetylase (NuRD) complex. We show that many NuRD components interacted with pericentrin by coimmunoprecipitation and that they localized to centrosomes and midbodies. Overexpression of the pericentrin-binding domain of CHD4 or another family member (CHD3) dissociated pericentrin from centrosomes. Depletion of CHD3, but not CHD4, by RNA interference dissociated pericentrin and γ-tubulin from centrosomes. Microtubule nucleation/organization, cell morphology, and nuclear centration were disrupted in CHD3-depleted cells. Spindles were disorganized, the majority showing a prometaphase-like configuration. Time-lapse imaging revealed mitotic failure before chromosome segregation and cytokinesis failure. We conclude that pericentrin forms complexes with CHD3 and CHD4, but a distinct CHD3–pericentrin complex is required for centrosomal anchoring of pericentrin/γ-tubulin and for centrosome integrity.

INTRODUCTION

Centrosomes are the major microtubule organizing centers in animal cells and play a pivotal role in cell cycle progression, bipolar spindle formation, and cytokinesis (Doxsey et al., 2005). A centrosome consists of a pair of centrioles surrounded by a protein matrix or pericentriolar material (PCM). Pericentrin localizes to the PCM, and it is responsible for anchoring both regulatory and structural proteins at the centrosome (Doxsey et al., 1994). Several pericentrin-interacting proteins have been identified including GCP2 and -3 of the γ-tubulin ring complex (γ-TuRC) (Dictenberg et al., 1998; Zimmerman et al., 2004), the light intermediate chain of cytoplasmic dynein (Purohit et al., 1999), the kinases protein kinase (PK)A and PKCβII (Diviani et al., 2000; Chen et al., 2004; Zimmerman et al., 2004), CG-NAP/AKAP450 (Takahashi et al., 2002), DISC1 (Miyoshi et al., 2004), and PCM-1 (Li et al., 2001). Pericentrin and its homologues in yeast, Drosophila, and Aspergillus has been shown to be involved in microtubule and spindle organization and function in some systems (Kilmartin and Goh, 1996; Purohit et al., 1999; Flory et al., 2002; Kawaguchi and Zheng, 2004; Zimmerman et al., 2004; Miyoshi et al., 2006) but not others (Martinez-Campos et al., 2004). Pericentrin also seems to play a role in the assembly/maintenance of primary cilia and flagella (Jurczyk et al., 2004; Martinez-Campos et al., 2004; Mikule et al., 2007). Chromodomain helicase DNA-binding (CHD) proteins are related by the presence of two chromatin organization modifier domains (chromodomains), a SWI/SNF-type ATPase domain, and DNA-binding motif. Chromodomains (30–50 amino acids) mediate protein–DNA or protein–protein interactions (Brehm et al., 2004). The human CHD family contains at least nine members that can be grouped into subfamilies based on sequence homology: CHD1 and CHD2; CHD3, CHD4, and CHD5; and CHD6–CHD9 (Woodage et al., 1997; Aubry et al., 1998; Schuster and Stoger, 2002; Thompson et al., 2003; Flaus et al., 2006). Homologues of CHD proteins have been found in Saccharomyces cerevisiae, Schizosaccharomyces pombe, Drosophila melanogaster, Caenorhabditis elegans, and Mus musculus (von Zelewsky et al., 2000; Jae Yoo et al., 2002). A single CHD gene, CHD1, is present in S. cerevisiae, whereas S. pombe contains two genes, Hrp1 and Hrp3 (Jin et al., 1998; Tran et al., 2000; Yoo et al., 2000; Jae Yoo et al., 2002). C. elegans and D. melanogaster both possess at least two different CHD genes (Woodage et al., 1997). CHD4, CHD3, or both have been found in multiple complexes, including the nucleosome remodeling deacetylase (NuRD) complex, a second complex regulating the deacetylation and inactivation of p53, a third involved in loading cohesin onto chromatin (Wade et al., 1998; Zhang et al., 1998; Luo et al., 2000; Wang and Zhang, 2001; Hakimi et al., 2002), and a forth potentially involved in the DNA damage response and silencing genes involved regulating cell cycle progression (Schmidt and Schreiber, 1999). In addition to CHD4 (and CHD3), the NuRD complex contains: histone deacetylases 1 and -2, retinoblastoma-associated proteins 46 and 48 (RbAp46/48), methyl-CpG-binding domain-containing protein 3 (MBD3), and a metastasis-associated protein (MTA) subunit (Tong et al., 1998; Wade et al., 1998; Zhang et al., 1998; Bowen et al., 2004). CHD4 hydrolyzes ATP in a DNA-dependent manner in vitro, and this activity is greatly increased when DNA is wrapped around

histone octamers (nucleosomes) (Wang and Zhang, 2001). This activity is thought to be important for the complex to act as a transcriptional repressor, perhaps by using energy of ATP hydrolysis to remodel nucleosomes. This could allow HDACs to access and deacetylate histone acetyl-lysine residues, thereby compacting nucleosomes and initiating transcriptional repression. A NuRD complex containing MTA3 was identified that regulates E-cadherin expression by controlling the expression of the negative regulator Snail (Fujita *et al.*, 2004), thus identifying the first gene regulated by the NuRD complex. It is unclear whether the NuRD is a global repressor or a repressor of a subset of genes. The NuRD complex characterized by Fujita *et al.* (2004), which contained MTA3 exclusively, suggests that MTA subunits might confer targeting specificity to the complex and that the activity of the NuRD might be restricted to the repression of specific genes. In this article, we identify an interaction between pericentrin and CHD3/4 and other NuRD components, and we suggest that these proteins form complexes distinct from the NuRD. We show that CHD3, CHD4, and MTA2 are components of the centrosome and that functional abrogation of CHD3, and to some extent CHD4, disrupts centrosome integrity and function, microtubule organization, and mitotic progression.

MATERIALS AND METHODS

Yeast Two-Hybrid Screen

The yeast strain AH109 was transformed with a GAL4 DNA-binding domain fusion vector, pGBKT7 (Clontech, Mountain View, CA), containing residues 1340-1756 of murine pericentrin. After determining that the GAL4 DBD/pericentrin fusion failed to autotransactivate the reporter genes, a 50-ml culture was grown overnight and then mated with the yeast strain Y187, which had been pretransformed with a human testes cDNA library (Clontech). Diploid clones were plated out onto to synthetic defined medium lacking leucine, tryptophan, histidine, and adenine to select for positive interactants.

cDNA Clones, Cloning Techniques, and Expression Constructs

cDNAs encoding CHD3, CHD4, and pericentrin were obtained from the following sources: CHD3 C-terminal sequence was from molecular analysis of genomes and their expression (IMAGE) clone 642405 (IMAGE consortium); CHD4 human testis cDNA library described above; and murine pericentrin as described previously (Purohit *et al.*, 1999). Sequences encoding pericentrin, CHD3, and CHD4 were amplified by polymerase chain reaction (PCR) by using *Pfu* Turbo DNA polymerase (Stratagene, La Jolla, CA), cloned into a donor vector of the Creator system (Clontech), and sequenced to verify the fidelity of the amplifying enzyme (Applied Biosystems, Foster City, CA). Coding sequences were transferred, by Cre-mediated recombination, into a range of expression vectors that included pLP-GBK-T7 (Clontech), pLP-CMV-myc (Clontech), and an existing FLAG-tagged vector that was converted for use with the system. The recombination protocol was as follows: 200 ng of each vector (donor and acceptor) were incubated at 37°C for 1 h in 1× Cre recombinase buffer with 1 U of Cre recombinase (New England Biolabs, Ipswich, MA), the enzyme was then heat inactivated at 70°C for 5 min, and the reaction was allowed to slowly cool to room temperature. Chemically competent DH5α were transformed with 2 μl of heat-inactivated recombination reaction.

Cell Culture and Transfection

COS and HeLa cells were cultured in DMEM supplemented with L-glutamine and 10% fetal calf serum, whereas retinal pigment epithelial (RPE)-1 cells (Clontech) were cultured in DMEM-F-12 supplemented with L-glutamine, sodium bicarbonate, and 10% fetal calf serum (Invitrogen). Cells were transfected either with Lipofectamine (Invitrogen, Carlsbad, CA) or by calcium phosphate precipitation. COS were transiently transfected with 5 μg of DNA by using Lipofectamine Plus reagent (Invitrogen) according to the protocol provided by the manufacturer. For immunofluorescent studies, 4×10^6 HeLa or RPE cells were electroporated with 20 μg of plasmid DNA in 500 μl of electroporation buffer (50 mM HEPES, pH 7, and 100 mM NaCl in phosphate-buffered saline (PBS) by using a Gene Pulser II electroporator (Bio-Rad, Hercules, CA) with a capacitance of 975 μF and a voltage of 290 V. Cells were plated out onto coverslips coated with 1 μg/μl fibronectin (Sigma-Aldrich, St. Louis, MO) and 5 μg/μl collagen, and they were fixed at various times with −20°C methanol.

Antibodies

The following antibodies were used either for immunofluorescent staining or Western blotting purposes: anti-pericentrin (M8) rabbit polyclonal (Doxsey *et al.*, 1994), anti-pericentrin B (gift from Trisha Davis as used in Mikule *et al.*, 2007), anti-RbAp46 (Abcam, Cambridge, MA), anti-CHD3 (Orbigen, San Diego, CA), anti-CHD3 (gift from W. Wang) anti-CHD4 (Orbigen), anti-CHD3/4 and anti-MTA2 (gifts from P. Wade). Secondary antibodies for immunofluorescent staining were obtained from the following sources: anti-mouse Alexa 488, anti-mouse AMCA and anti-rabbit Alexa 488 (all from Invitrogen); anti-mouse Cy3, anti-rabbit Cy3, and anti-human Cy5 (all from Jackson ImmunoResearch Laboratories, West Grove, PA). Horseradish peroxidase-linked anti-mouse and anti-rabbit secondary antibodies for Western blotting purposes were obtained from GE Healthcare (Little Chalfont, Buckinghamshire, United Kingdom).

Immunoprecipitations and Western Blotting

Before lysis, cells were briefly washed with PBS, placed on ice, and excess medium was removed by aspiration. Cells were lysed in either a low-stringency buffer (50 mM Tris-HCl, pH 7.5, 150 mM NaCl, 10 mM Na$_2$HPO$_4$, 1 mM EDTA, pH 8, and 1% Triton X-100) or a high-stringency buffer (50 mM Tris-HCl, pH 7.5, 150 mM NaCl, 1% sodium deoxycholate, 1% Triton X-100, and 0.1% SDS). Lysates were cleared by centrifugation at 14, 000 rpm for 10 min at 4°C and then added to antibodies that had been incubated with 25 μl of protein A/G beads (Santa Cruz Biotechnology, Santa Cruz, CA) for 30 min on ice. Proteins were immunoprecipitated overnight at 4°C with gentle mixing, the beads washed were five times with low-stringency lysis buffer, and then they were resuspended in 50 μl of 2X SDS sample buffer. Proteins were denatured at 90°C for 3 min, fractionated on SDS polyacrylamide gels, and transferred to Immobilon membrane (GE Healthcare). Membranes were blocked with 01.% Tween 20, 5% nonfat dried milk in PBS for 1 h at room temperature, and incubated with primary antibodies diluted either in the same buffer or 5% bovine serum albumin (BSA), PBS, and 0.1% Tween 20 for 2 h at ambient temperature or overnight at 4°C. Blots were washed four times with 0.1% Tween 20, 5% nonfat dried milk in PBS, incubated with secondary antibodies diluted in the same buffer for 1 h at ambient temperature, and washed three times with 0.2% Tween 20 in PBS. Revelation of blots was carried out using enhanced chemiluminescent development (Kirkegaard and Perry Laboratories, Gaithersburg, MD).

Immunofluorescence Staining

Cells were grown on 12-mm acid-washed circular coverslips and fixed with either −20°C methanol or 3.7% paraformaldehyde for 10 min at room temperature. Fixed cells were rehydrated by sequentially washing in PBS and then with a buffer consisting of PBS, 1% BSA, and 0.5% Triton X-100 (PBSA). Antibodies were diluted in PBSA, pipetted onto the surface of the coverslip, and incubated at room temperature for 1 h. The cells were washed with PBS, secondary antibodies diluted in the same buffer were added, and then cells were incubated for 30 min at room temperature. DNA was stained using 1 μg/ml 4,6-diamidino-2-phenylindole (DAPI) (Sigma-Aldrich).

Small-interfering RNA (siRNA)

The following duplexes were synthesized for the purpose of gene silencing: CHD3, AAGCGUGACAGUGAGGAGGAA and AAGGCCAUCGAUCGGU-UUAAU; CHD4, AAGGAUGAUGAUGAUGAUGAU and AACAGUUACC-AAGAAGACUUA; MTA2, AACCGGUAUAUUCAGCAGAAA; and lamin, AACUGGACUUCCAGAAGAACA (Dharmacon RNA Technologies, Lafayette, CO); pericentrin and green fluorescent protein (GFP) siRNA have been described previously (Mikule *et al.*, 2007). Cells were transiently transfected with siRNA at a final concentration of 200 nM by using oligofectamine (Invitrogen) according to the protocol provided.

Immunofluorescence Microscopy and Live Cell Imaging

Images of cells were taken using a Lecia microscope equipped a 100× objective lens and a CoolSNAP camera (Princeton Instruments). Deconvolution and fluorescence intensity measurements were carried out using MetaMorph software (Molecular Devices, Downingtown, PA) according to previously published protocols (Khodjakov and Rieder, 1999; Piehl *et al.*, 2004). Briefly, a 1-μm-diameter disk was placed over the centrosome, and the average fluorescence intensity was measured within this area. In cases where it was difficult to discern the location of the centrosome, regions were drawn onto an image of γ-tubulin staining and then copied and pasted onto the images to be measured. Live cell imaging was performed in 35-mm glass-bottomed dishes overlaying medium with mineral oil (Sigma-Aldrich). A heated chamber (Harvard Apparatus, Holliston, MA) perfused with CO$_2$ was used to maintain a temperature of 37°C, and constant pH. Images were taken every 5 min with an Olympus microscope fitted with a 20× objective lens.
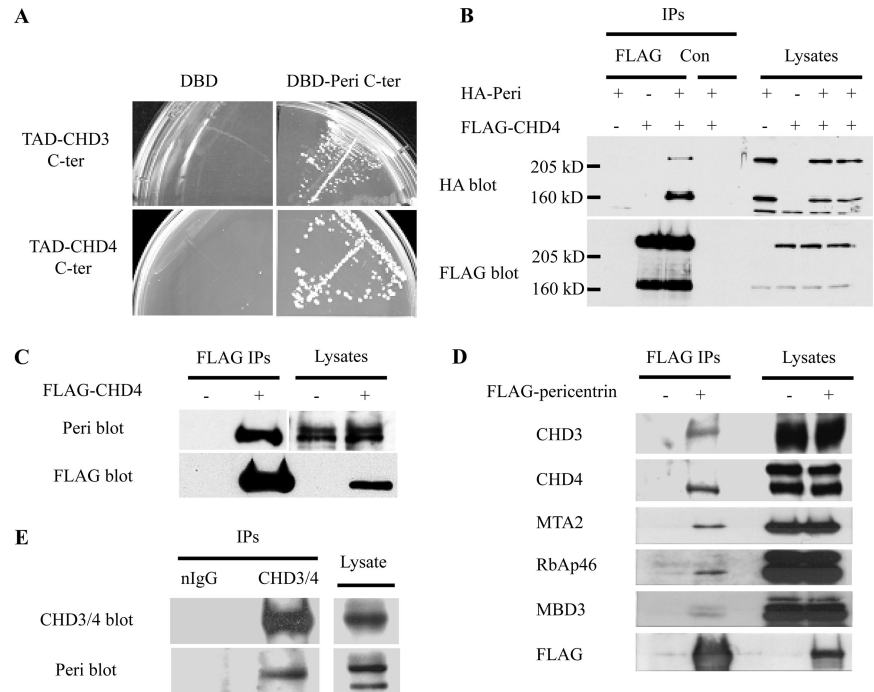
Figure 1. Components of the NuRD complex interact with pericentrin. (A) Yeast strain AH109, transformed with the C terminus of either CHD3 (residues 1566-1966) or CHD4 (residues 1577-1912) and a C-terminal (C-ter) region of pericentrin A (peri; residues 1340-1756) grown on selective media to demonstrate interactions (DBD, DNA binding domain; TAD, transactivation domain). (B) COS cells cotransfected with HA-pericentrin (HA-peri) and FLAG-CHD4 expression constructs. Anti-FLAG or anti-GFP (control; Con) were used for immunoprecipitations (IPs). IPs were immunoblotted (IB) with antibodies as indicated. (C) CoIP of endogenous pericentrin with FLAG-CHD4 from transfected COS cell lysates. (D) Immunoblots with antibodies to CHD3, CHD4, MTA2, RpAp46, MBD3, and FLAG after IP of FLAG-tagged pericentrin expressed in COS cells. (E) CHD3/4 was immunoprecipitated from HeLa cell lysates and immunoblotted for pericentrin or CHD3/4.

RESULTS

Identification of CHD3 and CHD4 as Pericentrin-interacting Proteins

To identify pericentrin-interacting proteins a region of mouse pericentrin A, corresponding to residues 1340-1756 (Zimmerman *et al.*, 2004), was used as bait in the yeast two-hybrid system to screen a human testis cDNA expression library. Among the pericentrin-interacting clones identified was the C-terminal domain of CHD4 (residues 1577-1912), a member of a protein family that localizes to the nucleus, functions in transcriptional regulation and contains two chromodomains and a SWI/SNF helicase domain (Woodage *et al.*, 1997). CHD3, a closely related member of the chromodomain-SWI/SNF helicase family, also interacted with pericentrin in the two-hybrid system (Figure 1A, residues 1566-1966). Deletion-mapping (Supplemental Figure S1) showed that two pericentrin-interacting domains existed between residues 1577-1733 and 1783-1912 within the C-terminal fragment of CHD4 isolated in the yeast two-hybrid screen. Sequence comparison of the C-terminal pericentrin-interacting region of CHD4 with that of CHD3 indicated that these regions share 59% sequence identity and 72% similarity. Immunoprecipitation experiments confirmed the two-hybrid interactions. In COS-7 cells transiently expressing hemagglutinin (HA)-tagged-pericentrin and FLAG-tagged-CHD4, immunoprecipitation of FLAG-CHD4 coprecipitated HA-pericentrin (Figure 1B). The observed pericentrin doublet likely represents a cleavage product (Golubkov *et al.*, 2005a,b). We then showed that overexpressed FLAG-CHD4 coprecipitated endogenous pericentrin (Figure 1C), and conversely, that overexpressed FLAG-tagged pericentrin coprecipitated endogenous forms of both CHD3 and CHD4 (Figure 1D); the top band of the CHD4 doublet could represent a posttranslationally modified form of the protein, potentially sumoylation, because this has recently been demonstrated to occur in vitro (Gocke *et al.*, 2005). Finally, immunoprecipitation of endogenous CHD3 and CHD4 from HeLa cell extracts coprecipitated endogenous pericentrin (Figure 1E). Other NuRD components were tested for their ability to interact with pericentrin. FLAG-tagged pericentrin expressed in COS cell coprecipitated a significant amount of the soluble MTA2 and less of the soluble RpAp46 and MBD3. It is possible that RpAp46 and MBD3 interact with pericentrin with a lower affinity or that they are transiently associated with the pericentrin–CHD3/4 complex.

NuRD Components Localize to the Centrosome

It has been shown that a number of NuRD complex components localize to the centrosome/spindle pole during mitosis, including CHD3/4 (Mi2), MBD3, and HDAC1 (Chadwick and Willard, 2002; Sakai *et al.*, 2002). We reexamined these results by investigating localization of NuRD components throughout the cell cycle in RPE-1 cells by using antibodies specific for CHD3, CHD4, MTA2, and RpAp46 (Figure 2, A–D). The predominant location of all proteins in interphase was the nucleus and to a lesser extent, the cytoplasm, but we also detected distinct staining of CHD3, CHD4, and MTA2 at centrosomes (Figure 2, A–C, respectively). This staining was enhanced when the cytoplasm was extracted with detergent before fixation (data not shown). During prophase the staining intensity of CHD3, CHD4, and MTA2 diminished in the nucleus. Centrosome staining of CHD3 and MTA2 remained throughout mitosis, whereas the majority of the centrosomal CHD4 seemed to dissociate; CHD3/4 and MTA2 also occurred at the midbody during cytokinesis. RpAp46 did not localize to the centrosome at any cell cycle stage, but it was enriched on the spindle during metaphase (Figure 2D, middle). To determine whether NuRD components were core components of centrosomes or whether they simply accumulated at the minus ends of microtubules, we examined their localization in the presence of the microtubule depolymerizing drug nocodazole. In the absence of centrosomal microtubules CHD3, CHD4, and MTA2 retained their association with the centrosome in interphase and mitosis, demonstrating a stable interaction with this organelle (data not shown).
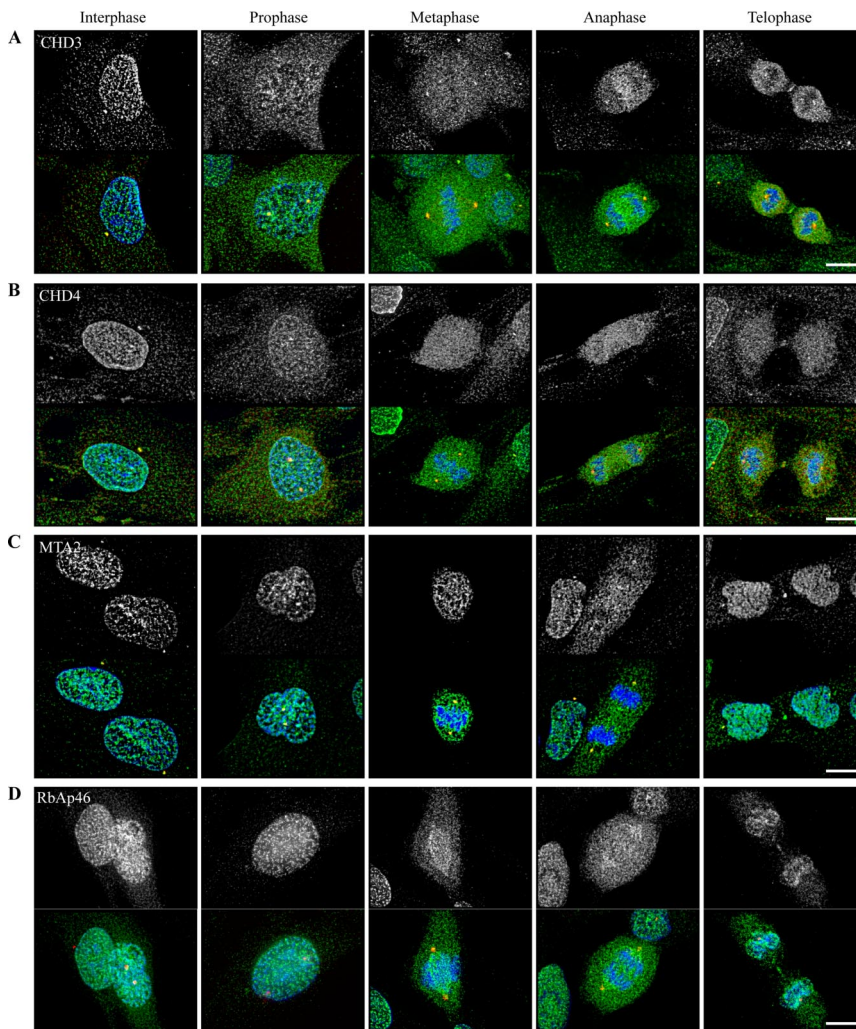
Figure 2. NuRD components localize to centrosomes and midbodies. (A–D) RPE-1 cells at the indicated cell cycle stages were stained with antibodies against the NuRD components CHD3 (A), CHD4 (B), MTA2 (C), and RbAp46 (D) (green), a centrosomal marker (γ-tubulin or human autoimmune serum 5051; red) and DAPI (DNA; blue). Antibodies to all NuRD components except RbAp46 stained centrosomes of interphasic cells. CHD3 and MTA2 centrosomal staining was observed at all mitotic stages, whereas CHD4 seem to dissociate from the centrosome during mitosis. Central spindle and midbody staining during anaphase and telophase was also observed. Bars, 10 μm.

Expression of the C Termini of CHD3 and CHD4 Displaces Centrosomal Pericentrin

Pericentrin acts a scaffold for the γ-TuRC and kinases such as PKA and PKCβII at the centrosome (Dictenberg *et al.*, 1998; Young *et al.*, 2000; Takahashi *et al.*, 2002; Chen *et al.*, 2004; Zimmerman *et al.*, 2004). To test whether pericentrin served as a centrosomal scaffold for CHD3/4 and other NuRD components, we attempted to disrupt the pericentrin–CHD3/4 interaction by expressing the pericentrin-interacting C-terminal domains of CHD3 and CHD4 (CT-CHD3 and -CHD4) in HeLa cells. We unexpectedly found that pericentrin (not CHD3/4) was mislocalized from centrosomes under these conditions (Figure 3). A significant percentage (63–70%) of CT-CHD3– or CT-CHD4–expressing cells contained no detectable centrosomal pericentrin (Figure 3B) or stained weakly possessing a tiny focus of pericentrin staining. In contrast, control cells expressing GFP mostly showed robust pericentrin staining that appeared as one or two foci. The dramatic loss of centrosomal pericentrin occurred rapidly (within 6 h) after electroporation of cDNA encoding CT-CHD3, indicating that transcriptional activity of the NuRD complex may not play a major role in the centrosome disruption phenotype. In some cells, overexpressed CT-CHD3 and CT-CHD4 localized to the centrosome, and these centrosomes showed a concomitant reduction in centrosomal pericentrin. This suggested that centrosomal recruitment of overexpressed CT-CHD3 and -CHD4 displaced or prevented the localization of pericentrin at this site. Together these results indicate that the C termini of CHD3 and CHD4 contain a functional pericentrin-binding domain.

siRNA-mediated Depletion of CHD3 Mislocalizes Centrosome Proteins

We next examined the effect of depleting CHD3 and CHD4 on centrosome integrity. siRNA targeting CHD3 or CHD4 showed depletion of the target protein by immunoblotting; other NuRD components were not affected (Figure 4A). Immunofluorescence analysis showed that target proteins were partially depleted from nuclei and lost from centrosomes in interphase cells (Figure 4, B and C). Cells depleted of CHD3 showed reduced centrosomal staining with 5051, a patient autoimmune serum that recognizes several centrosome proteins, including pericentrin (Doxsey *et al.*, 1994) and centriolin (Gromley *et al.*, 2003), indicating that these proteins were lost from the centrosome (Figure 4B). Fluorescence intensity measurements of centrosomal 5051 and CHD3/4 labeling indicated that RNA interference (RNAi) of the CHD3 gene resulted in a significant reduction in 5051 levels at the centrosome ($p < 0.001$, two-tailed test). In comparison, 5051 levels were only slightly reduced after treatment with CHD4 siRNA ($p < 0.05$) (Figure 4, D and E).
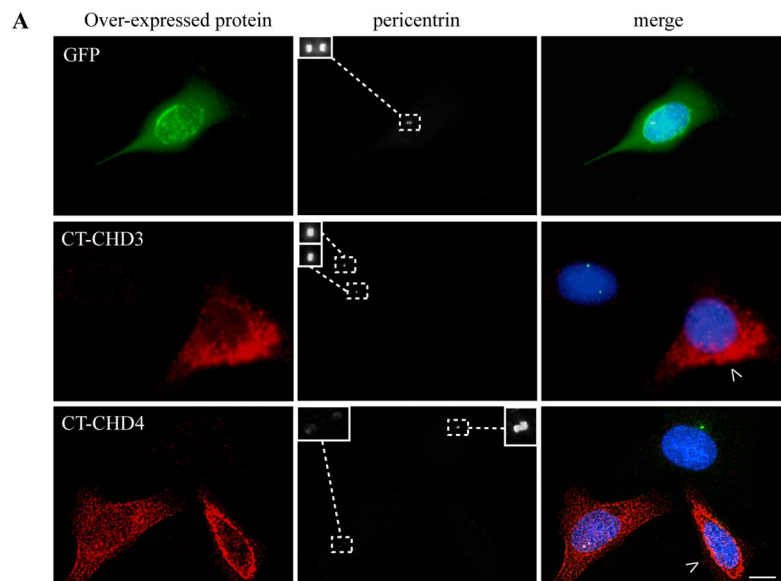
Figure 3. Overexpression of the C terminus (CT) of CHD3 or CHD3 induces loss of pericentrin from centrosomes in interphase cells. (A) HeLa cells electroporated with myc-tag constructs expressing the C terminus of CHD3 or CHD4 or a control plasmid (GFP), plated onto fibronectin/collagen-coated coverslips, fixed in −20°C methanol 6 h later, and stained with anti-myc to detect overexpressed protein (red) or pericentrin (green) with the exception of GFP control where transfected cells were stained with an anti-pericentrin antibody and a Cy3 secondary (red). In most cases, pericentrin was either undetectable (at arrowheads) or reduced at centrosomes (boxes) in cells expressing CT-CHD3 or CT-CHD4 compared with control GFP-expressing cells (row 1) or nontransfected cells (column 2). In some cases, overexpressed CT-CHD4 localized to the centrosome (left cell). Insets show enlargements of boxes. (B) Quantification of results from A show that ~70% of CT-CHD3/4-expressing cells have barely detectable pericentrin with centrosomal levels being 50% lower than the average (< average). The remainder possessed more than 50% of the average centrosomal pericentrin level (> average). Bar, 10 μm.

In fact, pericentrin immunofluorescence images and quantitative analysis showed that pericentrin was lost from centrosomes in cells depleted of CHD3 ($p < 0.001$; Figure 5, A and B). Surprisingly, increased centrosomal pericentrin levels were observed in cells treated with siRNA targeting CHD4 compared with lamin A/C siRNA-treated control cells ($p < 0.001$; Figure 5, A and B). Other experiments demonstrated that the level of γ-tubulin, a centrosome protein that binds pericentrin through its association with the γ-tubulin ring complex (Zimmerman *et al.*, 2004), was significantly reduced at the centrosome upon treatment with siRNA against CHD3 ($p < 0.001$), whereas a marginally significant reduction was observed upon CHD4 siRNA treatment ($p < 0.05$). This suggested that disruption of centrosomal pericentrin displaced a fraction of γ-tubulin from interphase centrosomes (Zimmerman *et al.*, 2004) and that other proteins likely anchor the remaining fraction of γ-tubulin to interphase centrosomes (Takahashi *et al.*, 2002). Centrin-1 staining in CHD3-depleted cells was not different from controls, indicating that the core structure of the centrosome (centrioles) was still intact (Figure 5E). These results, combined with those from transient transfection CHD3 and CHD4 C-termini, suggest that both proteins are able to interact with pericentrin. However, the data suggests that CHD3 is responsible for anchoring multiple components to the centrosome, including pericentrin, as siRNA-mediated depletion of the protein resulted in reduced centrosomal levels of pericentrin, γ-tubulin, and 5051 antigens. In contrast, loss of CHD4 resulted in increased centrosomal pericentrin levels, suggesting that this protein is a negative regulator and that it is involved in the displacement of pericentrin from the centrosome (Figure 5, A and B). It is likely that the overexpression of the CHD3/4 pericentrin-binding domains, which share 92% homology, disrupts the endogenous complexes at the centrosome, altering the balance of their activities and ultimately results in the loss of centrosomal proteins.

CHD3 Is Required for Centrosome Anchoring of Pericentrin and CHD4

It was clear from the above-mentioned experiments that centrosomal-anchoring of pericentrin was dependent upon the presence of CHD3; however, it was uncertain as to whether CHD3/4 required each other to associate with the centrosome. To address this question we silenced the CHD3 and CHD4 genes independently by RNAi, and we examined the localization pattern of each protein by using antibodies specific to CHD3 or CHD4 (Figure 6, A and B). The results
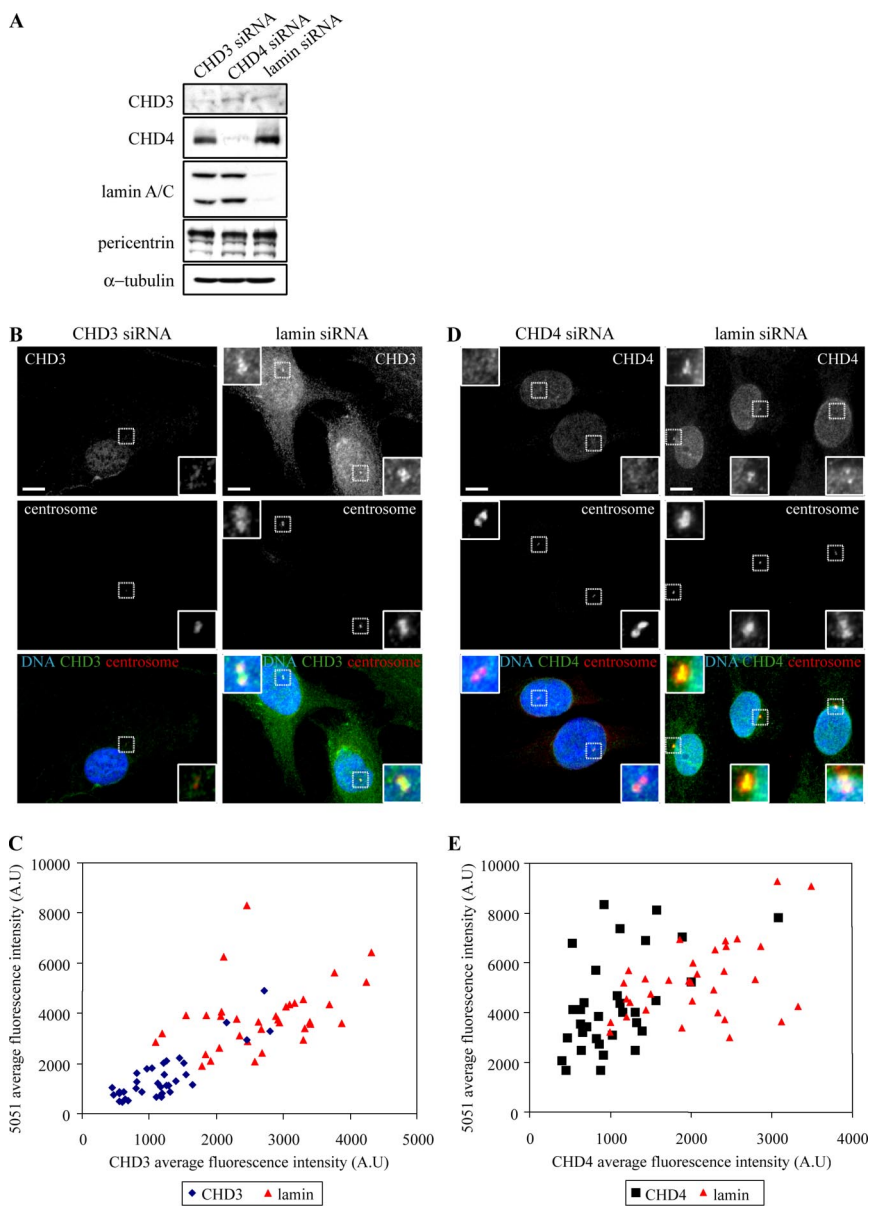
Figure 4. RNAi-mediated depletion of CHD3 but not CHD4 disrupts centrosome integrity. (A) RPE-1 cells treated with siRNAs targeting CHD3, CHD4 or lamin (control) for 72 h were lysed and IB for the indicated proteins. Note specific reduction of the targeted protein, but not others. Pericentrin levels unaffected under all conditions. (B and C) Cells treated with siRNAs targeting CHD3, CHD4, or lamin A/C were fixed in $-20°C$ methanol and stained with antibodies to CHD3, CHD4, or 5051 (centrosome marker). In many cells ($\sim$80%), CHD3 and CHD4 were depleted from nuclei and centrosomes. In cells depleted of CHD3, a decrease in 5051 autoantibody staining was observed (B, middle image of left column), suggesting a loss of many of the proteins known to react with this human autoimmune serum. In contrast, depletion of CHD4 did not show significant loss of 5051 staining (C, middle image of left column). (D and E) Results of fluorescence intensity measurements plotting centrosomal 5051 levels against those of CHD3 or CHD4. After siRNA-mediated silencing of the CHD3 gene, both CHD3 and 5051 levels were reduced compared with lamin A/C siRNA-treated control cells (average CHD3 levels after CHD3 RNAi, 1182.9 arbitrary units (a.u.); lamin A/C RNAi, 2715.3 a.u; average 5051 levels after CHD3 RNAi, 1433.7 a.u; lamin A/C RNAi, 3834.0 a.u.). A slight reduction in the level of centrosomal 5051 was observed after treatment with CHD4 siRNA (average CHD4 levels after CHD4 RNAi, 1050.1 a.u.; lamin A/C RNAi, 2070.8 a.u.; average 5051 levels after CHD4 RNAi, 4343.7 a.u.; lamin A/C RNAi, 5256.2 a.u.). Bars, 10 μm.

showed that CHD3 RNAi significantly depleted the fraction of CHD4 located at the centrosome but that it did not dramatically alter the localization pattern of CHD4 within the nucleus, as judged by centrosomal fluorescence intensity measurements ($p < 0.001$; Figure 6, A and C). In contrast, CHD4 RNAi seemed to have no effect upon the localization of CHD3 with the centrosomal and nuclear fractions remaining unperturbed. In support of this, fluorescence intensity measurements showed that there was no significant difference in the level of CHD3 at the centrosome after CHD4 RNAi compared with a lamin A/C RNAi control ($p > 0.05$; Figure 6D). These data combined with the results presented in Figure 5 suggest that CHD3 is a centrosomal protein essential for anchoring pericentrin and CHD4 to the centrosome. The data also indicate that CHD4 plays a role in negatively regulating the amount of pericentrin at the centrosome, because CHD4 RNAi resulted in increased centrosomal levels of pericentrin. It is interesting to note that the localization patterns of CHD3 and CHD4 differ slightly during mitosis, with CHD3 remaining associated with the cen-

trosome, whereas CHD4 seems to dissociate from the organelle. Thus, it is tempting to speculate that CHD4 is a factor controlling, in part, the mitotic accumulation of pericentrin at the centrosome. We next asked whether pericentrin depletion affected the centrosome localization of CHD3. In cells depleted of pericentrin no change in the centrosome levels of CHD3 were observed (Figure 7A). Quantification of these centrosomes showed that despite a significant decrease in pericentrin at centrosomes, CHD3 centrosome levels were only marginally reduced ($p < 0.001$; Figure 7B). This indicated that: CHD3-anchored pericentrin to centrosomes, pericentrin did not play a role in NuRD anchoring at the centrosome, and pericentrin and the NuRD complex were not mutually dependent in their centrosome localization.

Microtubule Organization and Regrowth Is Altered in CHD3 siRNA-treated Cells

CHD3/4-dependent mislocalization of centrosomal pericentrin and γ-tubulin, which both play a role in microtubule nucleation and organization (Zimmerman *et al.*, 2004), sug-
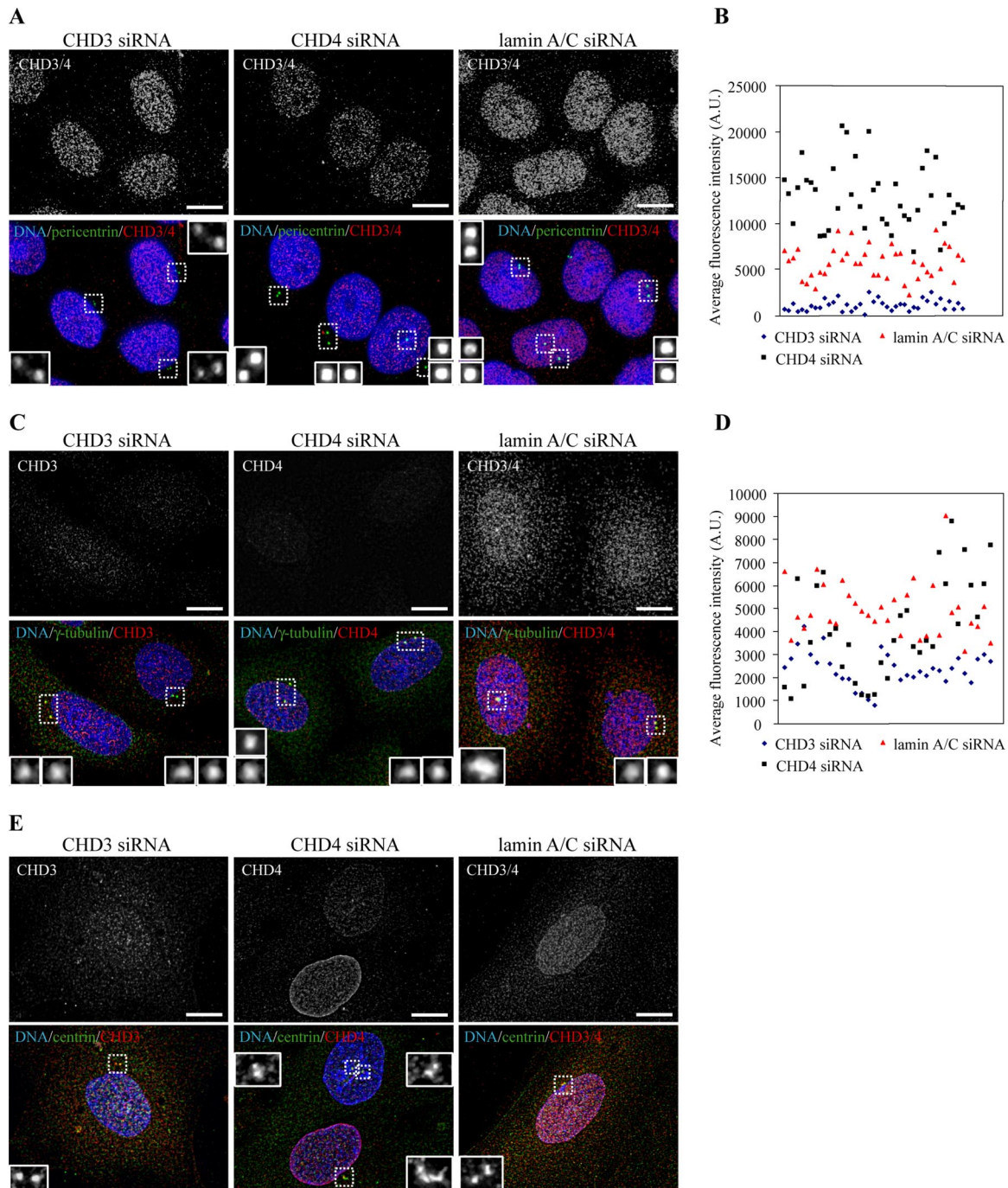
Figure 5. CHD3 depletion reduces centrosomal levels of pericentrin and γ-tubulin but not centrin. (A) HeLa cells treated with siRNAs against CHD3, CHD4, or lamin A/C (control) for 48 h were fixed in −20°C methanol and stained with antibodies to CHD3/4 (red) and pericentrin (green). Silencing of CHD3 (left) but not CHD4 or lamin (middle and right) induced loss of centrosomal pericentrin. (B) Results of fluorescent intensity measurements quantifying pericentrin levels showed that CHD3 RNAi induced a loss of pericentrin from the centrosome (p < 0.001), whereas levels were elevated after CHD4 RNAi (p < 0.001). Average centrosomal pericentrin levels were as follows: after CHD3 RNAi, 1142.9 a.u.; CHD4 RNAi, 12,964.1 a.u.; and lamin A/C RNAi 5784.6 a.u. (C) HeLa siRNA-treated cells from experiment in A were stained with antibodies to CHD3 or CHD4 (red) and γ-tubulin (green). Insets show enlarged images of centrosomal γ-tubulin. (D) Centrosomal γ-tubulin levels were quantified by taking fluorescence intensity measurements and found to be significantly reduced after CHD3 RNAi (p < 0.001). The γ-tubulin levels were only slightly reduced after CHD4 RNAi (p < 0.05 marginally significant). Average γ-tubulin levels were as follows: after CHD3 RNAi, 2408.7 a.u.; CHD4 RNAi, 4118.6 a.u., and lamin A/C RNAi, 4904.4 a.u. (E) RPE-1 cells treated with siRNAs as in A for 72 h were fixed and stained with antibodies to CHD3 or CHD4 (red) and centrin-1 (green) to label centrioles. Insets show enlarged images of centrin-1 staining, which was similar under all conditions. Bars, 10 μm.

gested a role for the NuRD complex in these processes. We first examined microtubule organization in cells expressing the C termini of CHD3 and CHD4 after nocodazole treatment and release. Six hours after electroporation of cDNAs
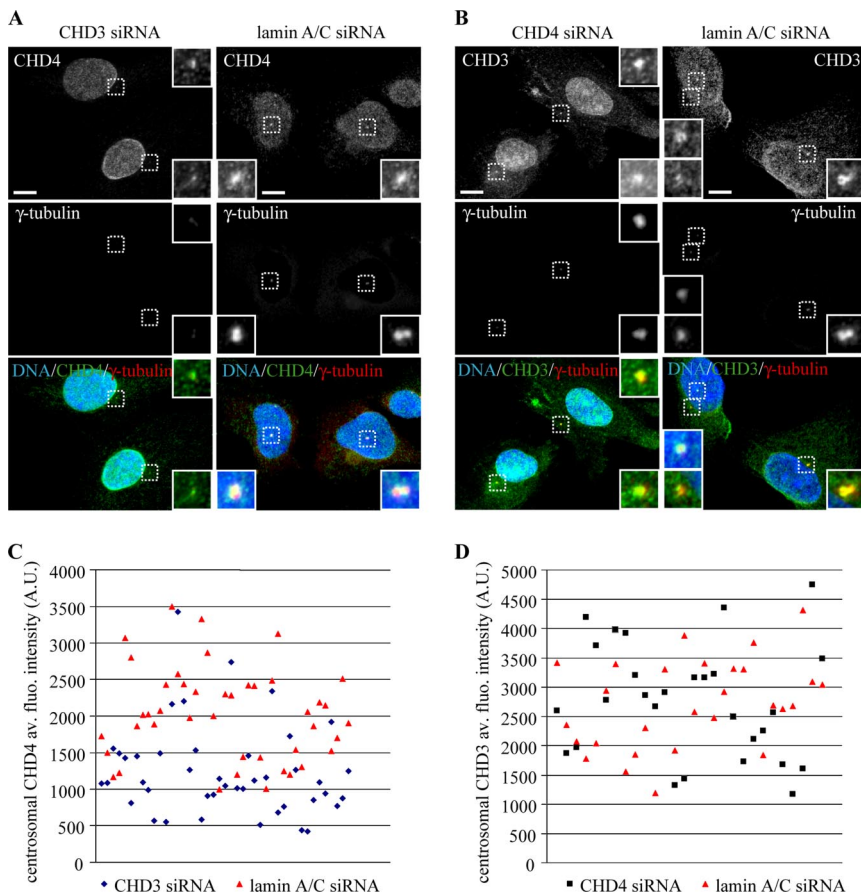
Figure 6. Anchoring of CHD4 to the centrosome is dependent upon CHD3. (A and B) RPE-1 cells were treated with siRNA against CHD3, CHD4, or lamin A/C for 72 h, fixed, and stained with either anti-CHD4 (A) or anti-CHD3 (B) and anti-γ-tubulin antibodies. (C) Fluorescence intensity measurements showed that silencing of the CHD3 gene resulted in a significant reduction in the amount of CHD4 at the centrosome (p < 0.001), but they did not seem to affect the nuclear pool of this protein. The average level of centrosomal CHD4 in lamin A/C control RNAi-treated cells was 2024.7 a.u. compared with 1234.5 a.u. in CHD3 RNAi-treated cells. (D) Cells treated with siRNA against CHD4 still possessed CHD3 at the centrosome with levels remaining unchanged compared with lamin A/C siRNA-treated controls (p > = 0.05). The average fluorescence intensities were 2756.0 a.u. and 2715.2 a.u. for CHD4 and lamin A/C siRNA-treated cells, respectively. Bars, 10 μm.

encoding the C termini of CHD3 or CHD4, microtubule organization was dramatically perturbed in 84% of RPE cells, whereas only 3% of GFP-transfected cells showed any change in microtubule organization (Figure 8A). Cells showed a dramatic reduction in the total number of microtubules, which usually formed a random meshwork rather than a radial array as seen in GFP-expressing controls. Moreover, the cells were more rounded compared with controls presumably due to disruption of the microtubule cytoskeleton. These data suggested that overexpression of the CHD3- or CHD4 C termini disrupted microtubule arrays by displacing centrosomal components and consequently compromising the ability of centrosomes to organize microtubule arrays. Profound defects in microtubule organization and microtubule nucleation were observed when CHD3 was depleted (Figure 8B). Sixty-three percent of CHD3 siRNA-treated cells showed phenotypes consistent with defects in microtubule nucleation, anchoring, and general organization. Because protein depletion occurs in only 75–80% of the cell population, the penetrance of the microtubule disruption phenotype seemed to be near complete. CHD3-depleted cells had microtubules that were fewer in number, not properly organized into radial arrays, and absent from large areas of the cytoplasm. In addition, a slight delay in nucleation was observed 5 min after nocodazole washout. Microtubules were sometimes organized into asters independent of centrosomes or formed bundles at the cell periphery, suggesting that they had been nucleated ectopically at these sites or that they were originally organized by centrosomes and subsequently released (Figure 7B). Centrosome-nucleated asters had fewer microtubules, many of which seemed

to have lost their centrosome attachment (Figure 8B, 5 min). When present, centrosome-anchored microtubules were as long as controls, suggesting that their polymerization rate was unaltered (Figure 8B and Supplemental Figure S3). Additional images of regrowing microtubules in CHD3 siRNA-treated cells are shown in Supplemental Figure S3. Microtubules were often found at the cell periphery unattached to centrosomes, suggesting that they had been nucleated ectopically at these sites or that they were centrosome nucleated, released, and transported to these sites (Supplemental Figure S3). Nuclei were often displaced from a central position presumably from loss of microtubule organization. Ten minutes after nocodazole washout, microtubules seemed to be dramatically curved at the cell periphery and often formed bundles around the nucleus (Figure 8B, bottom). Some CHD4-depleted cells exhibited poorly formed microtubule arrays (24%), a significantly higher percentage than lamin siRNA-treated cells (1–2%), but neither ectopic microtubule nucleation nor a delay in nucleation was observed after 5 min of regrowth.

CHD3 Depletion Causes Mitotic Defects and Cytokinesis Failure

We next investigated the effect of CHD3 depletion on mitotic spindle integrity and function. Reduction of CHD3 levels induced spindle defects in 59.6% of mitotic cells (Figure 9 and Supplemental Figure S2). The most prominent phenotype was a disrupted prometaphase-like configuration with a dramatic reduction in spindle microtubules and misalignment of chromosomes within spindles (Figure 9A). We also observed significant numbers of spindles in which the cen-
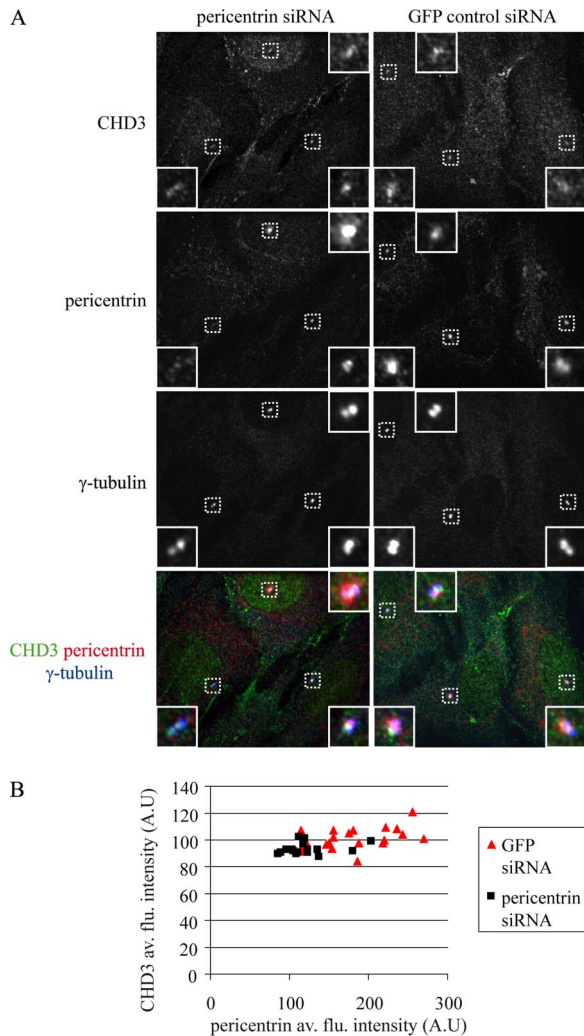
Figure 7. Pericentrin is not required for CHD3 centrosomal localization. (A) RPE-1 cells were treated with siRNA against pericentrin or GFP for 72 h, fixed, and stained with anti-CHD3 (green), anti-pericentrin (red) and anti-γ-tubulin (blue) antibodies. Insets show enlargements of the centrosomal areas marked with boxes. Depletion of pericentrin did not significantly alter the localization of CHD3 to the centrosome. (B) Quantification of pericentrin and CHD3 levels at the centrosome by measuring fluorescence intensity. Pericentrin levels were reduced upon RNAi, but CHD3 levels remained virtually unchanged. Bars, 10 μm.

trosomes had separated giving rise to a bipolar spindle, but only one pole seemed to nucleate microtubules (referred to as half-spindles in the legend of Figure 9). Monopolar spindles, tripolar spindles and lagging chromosomes were often observed. In contrast, such spindle defects were observed in only 3.6% of the control HeLa cell population (lamin A/C siRNA treated) and 14.4% in CHD4-depleted cells (Figure 9B). The percentage of spindle defects in CHD4-depleted cells was significantly higher than controls but less than CHD3-depleted cells, and it did not include the predominant prometaphase-like defects seen after CHD3 depletion. Consistent with the apparent loss of microtubule polymer in spindles of CHD3 depleted cells was a reduction in the amount of γ-tubulin at the spindle poles and on the spindle (Figure 9C). There seemed to be a selective loss of γ-tubulin from the poles as the total cellular level of the protein, assessed by immunoblotting, was similar to controls (data

not shown). Spindle pole levels of γ-tubulin in CHD4-depleted cells were similar to controls, suggesting that the modest increase in microtubule disorganization and spindle defects seen in these cells occurred by a mechanism distinct from the CHD3-induced defects. To further investigate the fate of CHD3-depleted cells during mitosis, we performed time-lapse imaging by using phase contrast microscopy. Cells were continuously examined for 23–28 h (Figure 10 and Supplemental Movies S1 and S2). Control cells (lamin A/C depleted) completed the transition from cell rounding to anaphase in 37.8 min, and 27/28 completed mitosis normally (Figure 10, A and D); one cell formed a tripolar spindle and gave rise to three progeny. In contrast, CHD3-depleted cells that completed cell division took an average of 265 min to transit the same time period. Many CHD3-depleted cells failed to segregate their chromatids, exited mitosis, and reattached to the substrate as mononuclear polyploid cells (Figure 10C). Others attempted to divide but failed in cytokinesis to form binucleated cells (Figure 10B). Whereas all control cells entered mitosis during the time that cells were examined, only half of the CHD3-depleted cells entered mitosis in the same time frame. This suggested a delay at a cell cycle stage before mitosis. CHD3-depleted cells that failed cytokinesis sometimes entered a second round of division. Defects at multiple stages of cytokinesis are consistent with general disorganization of microtubules in CHD3-depleted cells.

DISCUSSION

Identification of Novel Pericentrin-interacting Proteins
We have shown that pericentrin interacts with members of the NuRD complex and that the NuRD components CHD3, CHD4, and MTA2 localize to centrosomes during interphase. Differences in the localization patterns of NuRD components during mitosis were observed; CHD3 and MTA2 remained associated with the centrosome, whereas most of the CHD4 dissociated and was present at a reduced level from metaphase until telophase. Other NuRD components have been shown to localize to spindle poles (MBD3, HDAC1) (Chadwick and Willard, 2002; Sakai *et al.*, 2002), suggesting the entire complex may be located at this site, in addition to its nuclear localization.

Pericentrin–NuRD Complexes
Our results suggest that pericentrin interacts with a subset of NuRD components, indicating that this complex may be different from other NuRD complexes. There is some controversy within the chromatin field as to whether CHD3 is present within the NuRD complex. Zhang *et al.* (1998) isolated NuRD complexes from HeLa nuclear extracts and identified 43 peptides by mass spectrometric analysis, the majority of which corresponded to sequences conserved between CHD3 and CHD4, although four peptides specifically derived from CHD4 (Mi2β), but none from CHD3, were identified (Zhang *et al.*, 1998). Other groups found that CHD3 was present in the NuRD, but it was less abundant than CHD4, suggesting that CHD3 either formed distinct complexes or it was a minor component of the NuRD (Tong *et al.*, 1998; Wade *et al.*, 1998; Xue *et al.*, 1998). Together, these data suggest that pericentrin forms a complex with CHD3 that is distinct from the NuRD. Differences in the abundances of NuRD components within the pericentrin complex support this argument, because low amounts of MBD3 and RpAp46 were found to be present, suggesting that these were not core components or interacted weakly. Our data
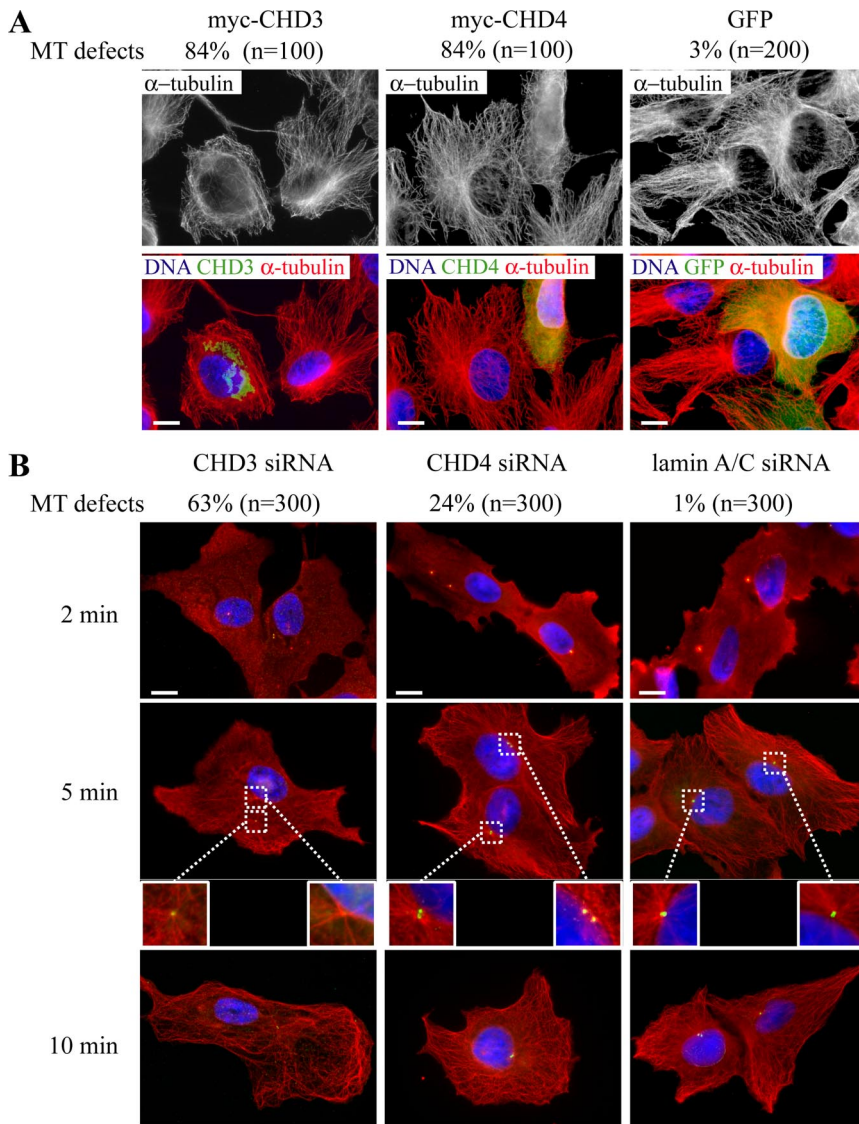
A

MT defects

myc-CHD3	myc-CHD4	GFP
84% (n=100)	84% (n=100)	3% (n=200)

B

MT defects

CHD3 siRNA	CHD4 siRNA	lamin A/C siRNA
63% (n=300)	24% (n=300)	1% (n=300)

Figure 8. Microtubule organization and nucleation is diminished in cells overexpressing or depleted of CHD3. (A) RPE-1 cells were electroporated with myc-tagged CHD3 or CHD4 C terminus or GFP as a control. Cells were fixed 6 h after transfection and stained with anti-α-tubulin and anti-myc antibodies. Cells transfected with either the C terminus of CHD3 or CHD4 possessed fewer and more disorganized microtubule arrays compared with GFP controls with 84%, in each case, exhibiting the phenotype shown. In contrast only 3% of GFP-transfected cells had a disorganized microtubule array. (B) Time course of microtubule regrowth. Cells depleted of CHD3, CHD4, or lamin (control) for 40 h were treated with nocodazole for 90 min; washed free of drug; fixed at 2-, 5-, and 10-min time intervals; and stained for microtubules (red), centrosomes (5051 autoimmune serum; green) and DNA (blue). Note fewer centrosome-nucleated microtubules (column 1, middle) and the curved, unfocused microtubules (column 1, bottom). One microtubule aster (right box, first column) is not associated with a centrosome. Percentages refer to number of cells having disrupted microtubule arrays. Bars 10 μm.

also indicate that CHD3 and CHD4 probably form different complexes with pericentrin, which have alternative functions. CHD3 seems to play a role in anchoring proteins at the centrosome both in interphasic and mitotic cells, whereas CHD4 seems to modulate the amount of protein at the centrosome, but it is not directly involved in protein anchorage at this site.

Does CHD3 Directly Anchor Pericentrin at Centrosomes?

Our transient transfection experiments support a direct role for CHD3/NuRD in anchoring pericentrin to the centrosome. The overexpression of the pericentrin-binding domains of either CHD3 or CHD4 displaced endogenous pericentrin from the centrosome within 6 h, a time that is likely too short to significantly alter gene expression. Furthermore, overexpressed proteins were distributed throughout the cytoplasm, and presumably they did not disrupt the function of the NuRD complex within the nucleus, because they did not localize to this cellular compartment. However, it is difficult to exclude an alternative model whereby expression of pericentrin or another protein associated with controlling pericentrin function is transcriptionally regulated by the

NuRD. Our results also demonstrate that pericentrin depletion does not perturb centrosomal CHD3, showing a lack of codependence in centrosome localization and providing further evidence for an anchoring function for CHD3.

A Link between the Centrosome and Nucleus?

The interaction between pericentrin, a centrosomal protein, and CHD3/4 and MTA2, components of a nuclear complex is not without precedence. This interaction joins a growing list of liaisons between nuclear and centrosomal proteins. For example, centrin-2 is part of the XPC, transforming acidic coiled-coil (TACC) proteins 1–3 directly bind to the histone acetyltransferase hGCN5L2, the *Drosophila* protein CP190 forms part of the gypsy chromatin insulator, and hEg5 is within an N-CoR repressor complex (Araki *et al.*, 2001; Yoon *et al.*, 2003; Gangisetty *et al.*, 2004; Pai *et al.*, 2004; Doxsey *et al.*, 2005). These complexes have a diverse range of functions. XPC is involved in nucleotide excision repair, and it is responsible for detecting damaged DNA in global genome nucleotide excision repair. The role of hEg5 within the N-CoR repressor complex, if it is a genuine component, is unknown. CP190 was found to be an essential component of
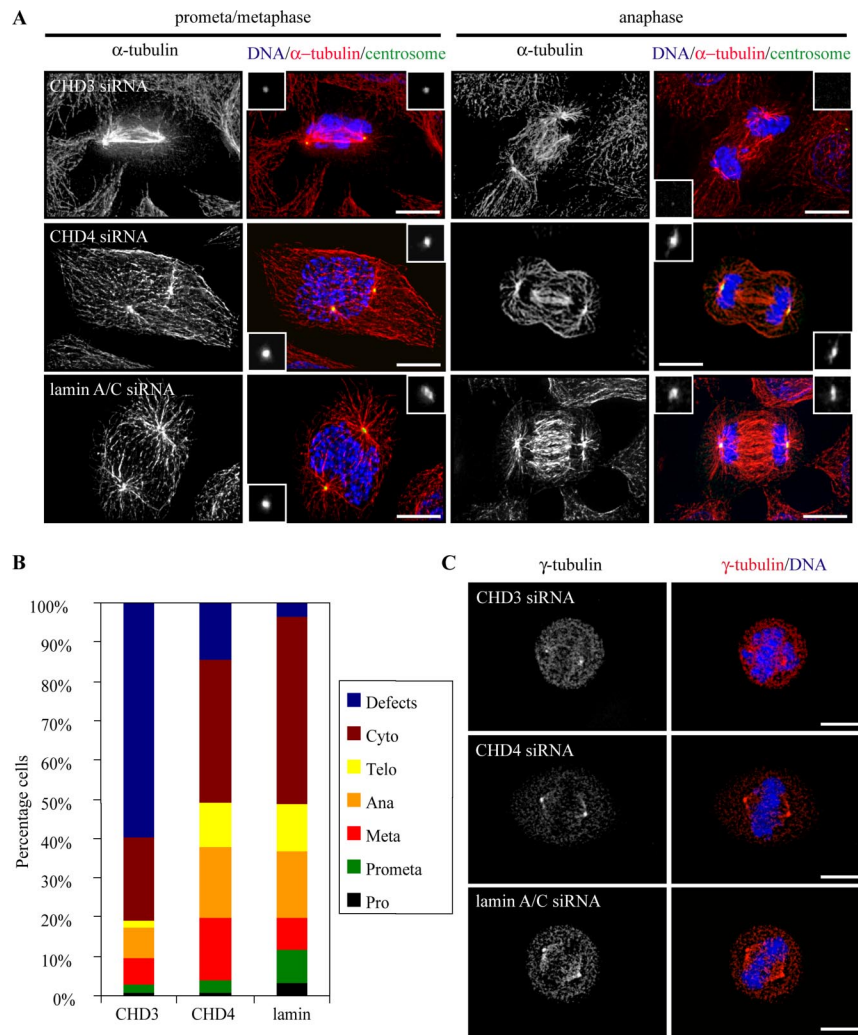
Figure 9. CHD3 depletion induces mitotic spindle defects. (A) HeLa cells treated with the indicated siRNAs for 48 h were fixed with −20°C methanol and stained with anti-α-tubulin (red) and 5051 (green, centrosomes) antibodies. CHD3 depletion (top) resulted in poorly organized spindles, misaligned chromosomes, and bundled microtubules compared with CHD4 and lamin A/C siRNA-treated cells (bottom). Also see Supplemental Figure 2. Insets, 5051-labeled centrosomes. (B) Quantification of spindle defects in siRNA-treated cells. Defects, which include abnormal prometaphase-like phenotype (specific for CHD3), monopolar-, tripolar-, and half-spindles and spindles with lagging chromosomes, are ~60% in CHD3-depleted cells. Other categories indicate the percentage of cells in each phase of mitosis that seem to be undergoing normal division (cyto, cytokinesis; telo, telophase; ana, anaphase; meta, metaphase; prometa; prometaphase; and pro, prophase). n = 100–200 mitotic cells counted for each condition. (C) γ-Tubulin staining in CHD3-depleted mitotic HeLa cells was reduced on poles and spindles and increased in the cytoplasm when compared with CHD4- and lamin AC-depleted cells. Bars, 10 µm.

the gypsy chromatin insulator and localizes to centrosomes, although mutation of this gene seemed to have no effect upon centrosome function (Pai *et al.*, 2004). Human TACC proteins localize to the nucleus and centrosome, although TACC1 and -3 associate with the centrosome only during mitosis (Gergely *et al.*, 2000). In contrast, TACC proteins are involved in microtubule organization, and they enhance recruitment of microtubules to the mitotic spindle (Gergely *et al.*, 2000). Alternatively, they seem to regulate gene expression via their interaction with the HAT hGCN5L2, which associates with chromatin remodeling components (Gangisetty *et al.*, 2004). Abnormal expression of TACC proteins contributes to the development of multiple myeloma, breast and gastric cancer, an effect that could occur via two different mechanisms, aberrant gene expression or spindle dysfunction (Gergely *et al.*, 2000; Conte *et al.*, 2002, 2003; Gangisetty *et al.*, 2004). Thus, there are clear parallels between TACC proteins and CHD3/4, because both have similar localization patterns, play roles in transcription regulation and alter microtubule patterns. Together, these results indicate that nuclear proteins play a role in regulating the activity of the centrosome.

Does Pericentrin Regulate Gene Expression?

RNAi experiments demonstrated that the nuclear protein CHD3 anchors pericentrin to the centrosome and affects

microtubule and spindle function, which provokes the question, Does the centrosome protein pericentrin function in the nucleus? A recent study demonstrated that cells treated with leptomycin B, an inhibitor of nuclear export, induced accumulation of pericentrin within the nucleus (Keryer *et al.*, 2003). This indicates that pericentrin is able to traverse the nuclear envelope but that it is rapidly shuttled out of this compartment and might have a function within the nucleus. Other evidence suggests a role for pericentrin in the nucleus. A NuRD complex containing MTA3 has recently been found to play a role in governing the expression of the E-cadherin by controlling the level of Snail, a transcriptional repressor of this gene. A cDNA encoding a protein sharing homology with the transcriptional repressor kaiso was also identified as a pericentrin-interacting protein in the yeast two-hybrid screen (Sillibourne and Doxsey, unpublished observation). If this kaiso-like protein is a bona fide interacting protein, it would further support the idea that pericentrin plays a role in regulating gene expression by associating with specific transcription factors and components of the NuRD complex. Moreover, a recent article demonstrating that pericentrin colocalizes with overexpressed SUMO in small nuclear dots suggests that pericentrin interacts with or is modified by the small ubiquitin modifier (SUMO) (Cheng *et al.*, 2006). In addition, there is evidence providing a link between SUMO and CHD3. A yeast two-hybrid screen for
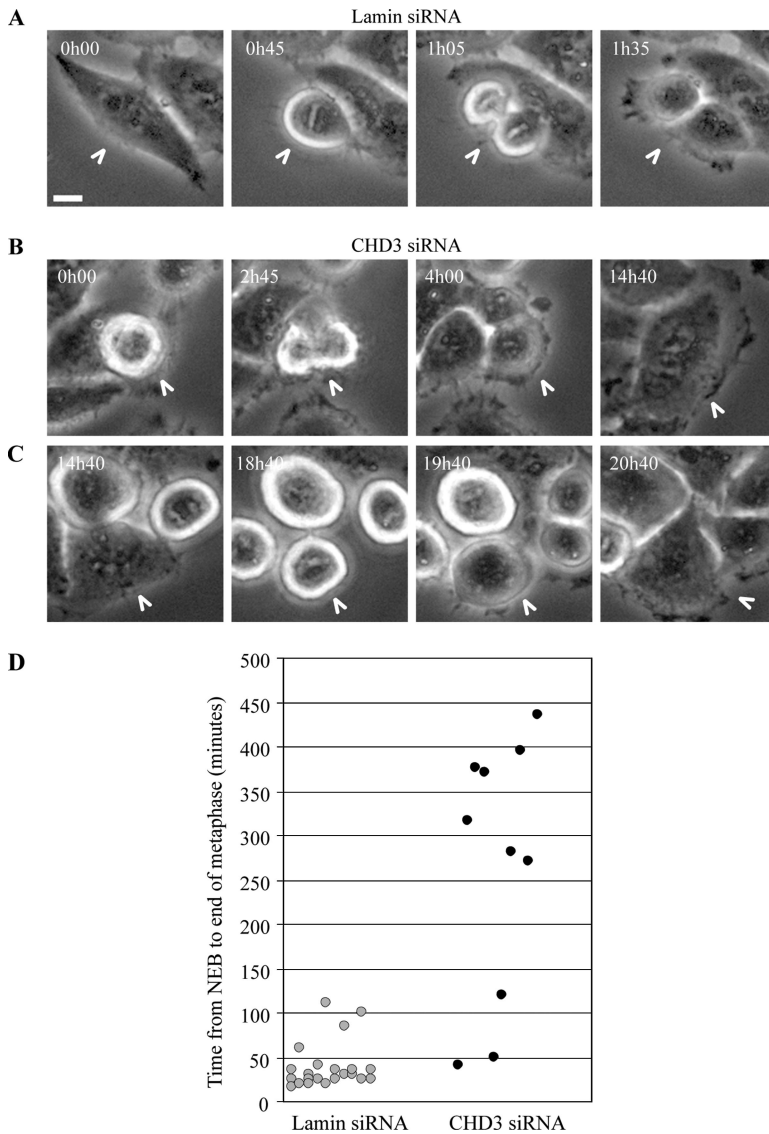
A

Lamin siRNA

B

CHD3 siRNA

C

D

Figure 10. CHD3 depletion causes metaphase delay, mitotic failure, and cytokinesis defects. Still images from time-lapse movies (see Supplemental Movies) of HeLa cells depleted of lamin A/C (A, control) or CHD3 (B and C). Image collection was initiated 24 h after siRNA treatment and continued for >22 h. (A) Successful mitosis in lamin A/C-depleted cell. (B) Mitotic CHD3-depleted cell (time 0 h 00 min) enters anaphase (2 h 45 min) and seems to complete telophase (4 h 00 min), but ultimately it fails cytokinesis to become a binucleated cell (14 h 40 min). (C) Another CHD3-depleted cell (arrowhead) enters metaphase (18 h 40 min) and exits mitosis without dividing (20 h 40 min). (D) Graph showing timing of individual cells from nuclear envelope breakdown (NEB) to anaphase onset: ~38 min in lamin A/C-depleted cells (range 15–110 min) and 265 min in CHD3-depleted cells (range 40–435 min). Bar, 10 μm.

p73-interacting proteins identified SUMO and CHD3 as potential partners; subsequent cross tests demonstrated that the C terminus of CHD3 interacted with SUMO (Minty *et al.*, 2000). CHD3 and CHD4 have been recently identified as a target of SUMO modification in vitro, indicating that these proteins are potentially modified in vivo (Gocke *et al.*, 2005). In this article, we have presented evidence demonstrating that CHD3/4 are centrosomal proteins and both play a role in controlling the amount of pericentrin, and possibly other components, at the centrosome. RNAi experiments indicate that ablation of CHD4 protein causes an increase in the amount of pericentrin anchored at the centrosome, suggesting that this protein is a negative regulator of pericentrin. In contrast, CHD3 RNAi reduces the amount of pericentrin at the centrosome, a surprising result given that CHD4 levels are also diminished by this treatment. More pericentrin would have been expected to localize to the centrosome after the CHD3 RNAi-induced loss of CHD4. This result suggests that CHD3 is a key centrosome component required for the anchoring of pericentrin, γ-tubulin, and CHD4 to the centrosome. We favor a model whereby CHD3 acts as a structural anchor keeping pericentrin and CHD4 at the centrosome and CHD4 is responsible for regulating or fine-tuning the removal of pericentrin from the centrosome. It is interesting to note that during mitosis CHD4 dissociates from the centrosome, whereas CHD3 remains associated, and pericentrin levels rise steadily throughout mitosis until entry into G1, upon which they fall dramatically. The dissociation of CHD4 from the centrosome is, perhaps, a prerequisite for the recruitment of pericentrin to the centrosome during mitosis. Several questions remain unanswered, including how is CHD3 anchored to the centrosome and how do CHD3 and CHD4 cooperate to regulate centrosome function? Finding the molecule to which CHD3 binds to at the centrosome may shed light on the function of this protein and help build a picture of the structural makeup of this multicomponent complex. How CHD4 regulates pericentrin levels at the centrosome is an open question, but it is tempting to speculate that posttranslational modification may play a role; perhaps through cycles of acetylation or decetylation or may be via SUMOylation. The answers to these questions will help to unravel the mechanism by which the helicases CHD3 and

CHD4 control the localization of their centrosomal partners and regulate centrosome function.

ACKNOWLEDGMENTS

REFERENCES

Araki, M., Masutani, C., Takemura, M., Uchida, A., Sugasawa, K., Kondoh, J., Ohkuma, Y., and Hanaoka, F. (2001). Centrosome protein centrin 2/caltractin 1 is part of the xeroderma pigmentosum group C complex that initiates global genome nucleotide excision repair. J. Biol. Chem. 276, 18665–18672.

Aubry, F., Mattei, M. G., and Galibert, F. (1998). Identification of a human 17p-located cDNA encoding a protein of the Snf2-like helicase family. Eur. J. Biochem. 254, 558–564.

Bowen, N. J., Fujita, N., Kajita, M., and Wade, P. A. (2004). Mi-2/NuRD: multiple complexes for many purposes. Biochim. Biophys. Acta 1677, 52–57.

Brehm, A., Tufteland, K. R., Aasland, R., and Becker, P. B. (2004). The many colours of chromodomains. Bioessays 26, 133–140.

Chadwick, B. P., and Willard, H. F. (2002). Cell cycle-dependent localization of macroH2A in chromatin of the inactive X chromosome. J. Cell Biol. 157, 1113–1123.

Chen, D., Purohit, A., Halilovic, E., Doxsey, S. J., and Newton, A. C. (2004). Centrosomal anchoring of protein kinase C betaII by pericentrin controls microtubule organization, spindle function, and cytokinesis. J. Biol. Chem. 279, 4829–4839.

Cheng, T. S., Chang, L. K., Howng, S. L., Lu, P. J., Lee, C. I., and Hong, Y. R. (2006). SUMO-1 modification of centrosomal protein hNinein promotes hNinein nuclear localization. Life Sci. 78, 1114–1120.

Conte, N., Charafe-Jauffret, E., Delaval, B., Adelaide, J., Ginestier, C., Geneix, J., Isnardon, D., Jacquemier, J., and Birnbaum, D. (2002). Carcinogenesis and translational controls: TACC1 is down-regulated in human cancers and associates with mRNA regulators. Oncogene 21, 5619–5630.

Conte, N., Delaval, B., Ginestier, C., Ferrand, A., Isnardon, D., Larroque, C., Prigent, C., Seraphin, B., Jacquemier, J., and Birnbaum, D. (2003). TACC1-chTOG-Aurora A protein complex in breast cancer. Oncogene 22, 8102–8116.

Dictenberg, J. B., Zimmerman, W., Sparks, C. A., Young, A., Vidair, C., Zheng, Y., Carrington, W., Fay, F. S., and Doxsey, S. J. (1998). Pericentrin and gamma-tubulin form a protein complex and are organized into a novel lattice at the centrosome. J. Cell Biol. 141, 163–174.

Diviani, D., Langeberg, L. K., Doxsey, S. J., and Scott, J. D. (2000). Pericentrin anchors protein kinase A at the centrosome through a newly identified RII-binding domain. Curr. Biol. 10, 417–420.

Doxsey, S. J., Stein, P., Evans, L., Calarco, P. D., and Kirschner, M. (1994). Pericentrin, a highly conserved centrosome protein involved in microtubule organization. Cell 76, 639–650.

Doxsey, S., Zimmerman, W., and Mikule, K. (2005). Centrosome control of the cell cycle. Trends Cell Biol. 15, 303–311.

Flaus, A., Martin, D. M., Barton, G. J., and Owen-Hughes, T. (2006). Identification of multiple distinct Snf2 subfamilies with conserved structural motifs. Nucleic Acids Res. 34, 2887–2905.

Flory, M. R., Morphew, M., Joseph, J. D., Means, A. R., and Davis, T. N. (2002). Pcp1p, an Spc110p-related calmodulin target at the centrosome of the fission yeast Schizosaccharomyces pombe. Cell Growth Differ. 13, 47–58.

Fujita, N., Jaye, D. L., Geigerman, C., Akyildiz, A., Mooney, M. R., Boss, J. M., and Wade, P. A. (2004). MTA3 and the Mi-2/NuRD complex regulate cell fate during B lymphocyte differentiation. Cell 119, 75–86.

Gangisetty, O., Lauffart, B., Sondarva, G. V., Chelsea, D. M., and Still, I. H. (2004). The transforming acidic coiled coil proteins interact with nuclear histone acetyltransferases. Oncogene 23, 2559–2563.

Gergely, F., Karlsson, C., Still, I., Cowell, J., Kilmartin, J., and Raff, J. W. (2000). The TACC domain identifies a family of centrosomal proteins that can interact with microtubules. Proc. Natl. Acad. Sci. USA 97, 14352–14357.

Gocke, C. B., Yu, H., and Kang, J. (2005). Systematic identification and analysis of mammalian small ubiquitin-like modifier substrates. J. Biol. Chem. 280, 5004–5012.

Golubkov, V. S., Boyd, S., Savinov, A. Y., Chekanov, A. V., Osterman, A. L., Remacle, A., Rozanov, D. V., Doxsey, S. J., and Strongin, A. Y. (2005a). Membrane type-1 matrix metalloproteinase (MT1-MMP) exhibits an important intracellular cleavage function and causes chromosome instability. J. Biol. Chem. 280, 25079–25086.

Golubkov, V. S., Chekanov, A. V., Doxsey, S. J., and Strongin, A. Y. (2005b). Centrosomal pericentrin is a direct cleavage target of membrane type-1 matrix metalloproteinase in humans but not in mice: potential implications for tumorigenesis. J. Biol. Chem. 280, 42237–42241.

Gromley, A., Jurczyk, A., Sillibourne, J., Halilovic, E., Mogensen, M., Groisman, I., Blomberg, M., and Doxsey, S. (2003). A novel human protein of the maternal centriole is required for the final stages of cytokinesis and entry into S phase. J. Cell Biol. 161, 535–545.

Hakimi, M. A., Bochar, D. A., Schmiesing, J. A., Dong, Y., Barak, O. G., Speicher, D. W., Yokomori, K., and Shiekhattar, R. (2002). A chromatin remodelling complex that loads cohesin onto human chromosomes. Nature 418, 994–998.

Jae Yoo, E., Kyu Jang, Y., Ae Lee, M., Bjerling, P., Bum Kim, J., Ekwall, K., Hyun Seong, R., and Dai Park, S. (2002). Hrp3, a chromodomain helicase/ATPase DNA binding protein, is required for heterochromatin silencing in fission yeast. Biochem. Biophys. Res. Commun. 295, 970–974.

Jin, Y. H. et al. (1998). Isolation and characterization of hrp1+, a new member of the SNF2/SWI2 gene family from the fission yeast Schizosaccharomyces pombe. Mol. Gen. Genet. 257, 319–329.

Jurczyk, A., Gromley, A., Redick, S., San Agustin, J., Witman, G., Pazour, G. J., Peters, D. J., and Doxsey, S. (2004). Pericentrin forms a complex with intraflagellar transport proteins and polycystin-2 and is required for primary cilia assembly. J. Cell Biol. 166, 637–643.

Kawaguchi, S., and Zheng, Y. (2004). Characterization of a Drosophila centrosome protein CP309 that shares homology with Kendrin and CG-NAP. Mol. Biol. Cell 15, 37–45.

Keryer, G., Di Fiore, B., Celati, C., Lechtreck, K. F., Mogensen, M., Delouvee, A., Lavia, P., Bornens, M., and Tassin, A. M. (2003). Part of Ran is associated with AKAP450 at the centrosome: involvement in microtubule-organizing activity. Mol. Biol. Cell 14, 4260–4271.

Khodjakov, A., and Rieder, C. L. (1999). The sudden recruitment of gamma-tubulin to the centrosome at the onset of mitosis and its dynamic exchange throughout the cell cycle, do not require microtubules. J. Cell Biol. 146, 585–596.

Kilmartin, J. V., and Goh, P. Y. (1996). Spc110p: assembly properties and role in the connection of nuclear microtubules to the yeast spindle pole body. EMBO J. 15, 4592–4602.

Li, Q., Hansen, D., Killilea, A., Joshi, H. C., Palazzo, R. E., and Balczon, R. (2001). Kendrin/pericentrin-B, a centrosome protein with homology to pericentrin that complexes with PCM-1. J. Cell Sci. 114, 797–809.

Luo, J., Su, F., Chen, D., Shiloh, A., and Gu, W. (2000). Deacetylation of p53 modulates its effect on cell growth and apoptosis. Nature 408, 377–381.

Martinez-Campos, M., Basto, R., Baker, J., Kernan, M., and Raff, J. W. (2004). The Drosophila pericentrin-like protein is essential for cilia/flagella function, but appears to be dispensable for mitosis. J. Cell Biol. 165, 673–683.

Mikule, K., Delaval, B., Kaldis, P., Jurczyk, A., Hergert, P., and Doxsey, S. (2007). Loss of centrosome integrity induces p38-p53-p21-dependent G1-S arrest. Nat. Cell Biol. 9, 160–170.

Minty, A., Dumont, X., Kaghad, M., and Caput, D. (2000). Covalent modification of p73alpha by SUMO-1. Two-hybrid screening with p73 identifies novel SUMO-1-interacting proteins and a SUMO-1 interaction motif. J. Biol. Chem. 275, 36316–36323.

Miyoshi, K., Asanuma, M., Miyazaki, I., Diaz-Corrales, F. J., Katayama, T., Tohyama, M., and Ogawa, N. (2004). DISC1 localizes to the centrosome by binding to kendrin. Biochem. Biophys. Res. Commun. 317, 1195–1199.

Miyoshi, K., Asanuma, M., Miyazaki, I., Matsuzaki, S., Tohyama, M., and Ogawa, N. (2006). Characterization of pericentrin isoforms in vivo. Biochem. Biophys. Res. Commun. 351, 745–749.

Pai, C. Y., Lei, E. P., Ghosh, D., and Corces, V. G. (2004). The centrosomal protein CP190 is a component of the gypsy chromatin insulator. Mol. Cell 16, 737–748.

J. E. Sillibourne *et al.*

Piehl, M., Tulu, U. S., Wadsworth, P., and Cassimeris, L. (2004). Centrosome maturation: measurement of microtubule nucleation throughout the cell cycle by using GFP-tagged EB1. Proc. Natl. Acad. Sci. USA *101*, 1584–1588.

Purohit, A., Tynan, S. H., Vallee, R., and Doxsey, S. J. (1999). Direct interaction of pericentrin with cytoplasmic dynein light intermediate chain contributes to mitotic spindle organization. J. Cell Biol. *147*, 481–492.

Sakai, H., Urano, T., Ookata, K., Kim, M. H., Hirai, Y., Saito, M., Nojima, Y., and Ishikawa, F. (2002). MBD3 and HDAC1, two components of the NuRD complex, are localized at Aurora-A-positive centrosomes in M phase. J. Biol. Chem. *277*, 48714–48723.

Schmidt, D. R., and Schreiber, S. L. (1999). Molecular association between ATR and two components of the nucleosome remodeling and deacetylating complex, HDAC2 and CHD4. Biochemistry *38*, 14711–14717.

Schuster, E. F., and Stoger, R. (2002). CHD5 defines a new subfamily of chromodomain-SWI2/SNF2-like helicases. Mamm. Genome *13*, 117–119.

Takahashi, M., Yamagiwa, A., Nishimura, T., Mukai, H., and Ono, Y. (2002). Centrosomal proteins CG-NAP and kendrin provide microtubule nucleation sites by anchoring gamma-tubulin ring complex. Mol. Biol. Cell *13*, 3235–3245.

Thompson, P. M., Gotoh, T., Kok, M., White, P. S., and Brodeur, G. M. (2003). CHD5, a new member of the chromodomain gene family, is preferentially expressed in the nervous system. Oncogene *22*, 1002–1011.

Tong, J. K., Hassig, C. A., Schnitzler, G. R., Kingston, R. E., and Schreiber, S. L. (1998). Chromatin deacetylation by an ATP-dependent nucleosome remodelling complex. Nature *395*, 917–921.

Tran, H. G., Steger, D. J., Iyer, V. R., and Johnson, A. D. (2000). The chromo domain protein chd1p from budding yeast is an ATP-dependent chromatin-modifying factor. EMBO J. *19*, 2323–2331.

von Zelewsky, T., Palladino, F., Brunschwig, K., Tobler, H., Hajnal, A., and Muller, F. (2000). The *C. elegans* Mi-2 chromatin-remodelling proteins function in vulval cell fate determination. Development *127*, 5277–5284.

Wade, P. A., Jones, P. L., Vermaak, D., and Wolffe, A. P. (1998). A multiple subunit Mi-2 histone deacetylase from *Xenopus laevis* cofractionates with an associated Snf2 superfamily ATPase. Curr. Biol. *8*, 843–846.

Wang, H. B., and Zhang, Y. (2001). Mi2, an auto-antigen for dermatomyositis, is an ATP-dependent nucleosome remodeling factor. Nucleic Acids Res. *29*, 2517–2521.

Woodage, T., Basrai, M. A., Baxevanis, A. D., Hieter, P., and Collins, F. S. (1997). Characterization of the CHD family of proteins. Proc. Natl. Acad. Sci. USA *94*, 11472–11477.

Xue, Y., Wong, J., Moreno, G. T., Young, M. K., Cote, J., and Wang, W. (1998). NURD, a novel complex with both ATP-dependent chromatin-remodeling and histone deacetylase activities. Mol. Cell *2*, 851–861.

Yoo, E. J., Jin, Y. H., Jang, Y. K., Bjerling, P., Tabish, M., Hong, S. H., Ekwall, K., and Park, S. D. (2000). Fission yeast hrp1, a chromodomain ATPase, is required for proper chromosome segregation and its overexpression interferes with chromatin condensation. Nucleic Acids Res. *28*, 2004–2011.

Yoon, H. G., Chan, D. W., Reynolds, A. B., Qin, J., and Wong, J. (2003). N-CoR mediates DNA methylation-dependent repression through a methyl CpG binding protein Kaiso. Mol. Cell *12*, 723–734.

Young, A., Dictenberg, J. B., Purohit, A., Tuft, R., and Doxsey, S. J. (2000). Cytoplasmic dynein-mediated assembly of pericentrin and gamma tubulin onto centrosomes. Mol. Biol. Cell *11*, 2047–2056.

Zhang, Y., LeRoy, G., Seelig, H. P., Lane, W. S., and Reinberg, D. (1998). The dermatomyositis-specific autoantigen Mi2 is a component of a complex containing histone deacetylase and nucleosome remodeling activities. Cell *95*, 279–289.

Zimmerman, W. C., Sillibourne, J., Rosa, J., and Doxsey, S. J. (2004). Mitosis-specific anchoring of {gamma} tubulin complexes by pericentrin controls spindle organization and mitotic entry. Mol. Biol. Cell *15*, 3642–3657.